Small-Angle Neutron Scattering Studies of Compatible Blends of Linear Poly(vinyl methyl ether) and Cross-Linked Deuterated Polystyrene

Barry J. Bauer,* Robert M. Briber, and Charles C. Han

Polymers Division, Institute for Materials Science and Engineering, National Bureau of Standards, Gaithersburg, Maryland 20899. *Received March 9, 1988; Revised Manuscript Received July 8, 1988*

ABSTRACT: Small-angle neutron scattering (SANS) from single-phase polymer blends of cross-linked deuterated polystyrene (PSD) and linear poly(vinyl methyl ether) (PVME) has been studied as a function of temperature. Phase separation during the polymerization resulted if the PVME present is greater than the amount which would swell the PSD network at equilibrium. SANS from the single-phase linear blend and the lowest cross-link density sample exhibited linear behavior for inverse zero-angle scattering, $S(0)^{-1}$, and inverse correlation length squared, ξ^{-2}, versus T^{-1} while the higher cross-link density sample showed pronounced curvature in the same plot, eventually crossing over the curves for the other two samples. Linear plots for $S(0)$ and ξ versus T^{-1} for the highest cross-link density single-phase sample could be obtained with the exponents $S(0)^{-0.57}$ and $\xi^{-1.44}$. The highest cross-link density single-phase sample was then deformed to $L/L_0 = 2.5$ and the SANS examined as a function of temperature. The scattering obtained was anisotropic wth different values of $S(0)$ and ξ in the directions parallel and perpendicular to the deformation. Plots of $S(0)^{-1}$ and ξ^{-2} versus T^{-1} indicated that the sample phase separated in the direction parallel to the deformation at a lower temperature than in the perpendicular direction.

Introduction

The effect of cross-links on the phase-separation behavior of miscible polymer blends is a topic that has not received much study or discussion in the literature. In a polymer blend of two components A and B there are three possible types of cross-links: A–A, B–B, and A–B. These cross-links may exist separately or in any combination. In this paper we will examine the effect of introducing A–A cross-links on the concentration fluctuations in the single-phase region of the phase diagram as studied by small-angle neutron scattering (SANS).[1] The effect of introducing all types of cross-links (A–A, B–B, and A–B) on the critical fluctuations and phase diagram will be addressed in a separate publication.[2]

The body of literature dealing with the study of interpenetrating polymer networks (IPNs) has addressed the issue of the cross-linking of polymer blends, but in the vast majority of the cases the systems studied were phase separated.[3-5] The only single-phase, miscible IPNs that have been reported are for polystyrene (PS) and poly(phenylene oxide) (PPO) by Frisch et al.[6] This study involved cross-linked polystyrene polymerized in the presence of cross-linked PPO resulting in two independent networks (only A–A and B–B cross-links). Evidence for miscibility was based on differential scanning calorimetry and dynamic mechanical measurements which showed a single glass transition temperature and electron microscopy which gave no evidence of phase separation. However, this system does not show a thermally induced phase separation transition before the onset of degradation for the blend of the linear polymers[7] and no attempt was made to determine the effect of cross-linking on the thermodynamics or single-phase stability. Coleman et al. have discussed other experimental evidence for single-phase IPNs and conclude that other than possibly for the PPO/PS system there is no conclusive evidence that miscible IPNs have been successfully made.[8]

There exists a complicated nomenclature for describing IPNs about which we will not go into detail except to note that the system described in our work would fall under the category of a semi-IPN (i.e., containing one cross-linked and one linear component).[3-6] By approaching the system in this paper as the study of a blend of linear B chains in a matrix of cross-linked A chains rather than as an "IPN", we hope to emphasize that we are interested, at least in this initial work, in the effect of cross-links on the concentration fluctuations in a single-phase system.

The phase-separation thermodynamics and critical phenomenon of the linear polymer blend of poly(vinyl methyl ether) (PVME) and polystyrene-d_8 (PSD) has been extensively studied by small-angle neutron scattering in this laboratory and elsewhere.[9-12] It has been shown that there is a temperature- and composition-dependent Flory interaction parameter, χ, which is negative at lower temperatures and increases with increasing temperature, becoming positive and resulting finally in phase separation and a lower critical solution temperature (LCST) at about 150 °C, depending on composition and molecular weight. The work presented in this paper represents the first attempt to synthesize a single-phase blend of cross-linked PSD with linear PVME and examine the effect of the cross-linking on the phase-separation behavior by small-angle neutron scattering (SANS) in comparison with that of the blend of the linear polymers.

Theoretical Background

Binder and Frisch have studied the thermodynamics of weakly cross-linked polymer blends containing A–A and/or B–B cross-links.[13] They modified the well-known Flory–Huggins formulation for the free energy of a polymer blend[14,15] by adding terms to account for the elastic energy of the polymer network. In formulating the free energy of a polymer blend containing A–A cross-links, we will follow their work explicitly.

The free energy per volume of an elastically deformed network, Δf, can be written as[13,16]

$$\frac{\Delta f}{kT} = \frac{\alpha\nu}{2}(\lambda_x^2 + \lambda_y^2 + \lambda_z^2 - 3) - \beta\nu \ln (\lambda_x\lambda_y\lambda_z) \quad (1)$$

where λ_i is the extension in the ith direction, ν is the number of elastically effective chains per volume, $\nu = 1/v_A N_{Ac}$, v_A is the molar volume of the repeat unit of polymer A, N_{Ac} is the number of repeat units of type A between crosslinks in the network, and α and β are constants that depend on the model of the network used to

* To whom correspondence should be sent.

derive eq 1. In the James and Guth theory[17] $\alpha = 1$ and $\beta = 0$ while according to Hermans[18] and Kuhn[19] $\alpha = 1$ and $\beta = 1$. Flory writes eq 1 with $\alpha = 1$ and $\beta = 2/f$ where f is the functionality of the junctions in the network.[20] In an isotropic system upon change of the volume fraction of the network from ϕ_s, the state where the network chains are completely relaxed, to a new composition ϕ the extension ratio, λ, can be written as

$$\lambda = (\phi_s/\phi)^{1/3} \tag{2}$$

For our purposes it will be assumed that the network is formed in the relaxed state, so ϕ_s will be assumed to be equal to the volume fraction at which the network was cross-linked. By substitution of the eq 2 into eq 1 and addition of the entropy of mixing term for a linear polymer (component B) of degree of polymerization N_B and a heat of mixing term containing the Flory interaction parameter χ, the free energy for the mixture can be written as

$$\frac{\Delta f}{kT} = \frac{3\alpha}{2\upsilon_A N_{Ac}}(\phi_s^{2/3}\phi^{1/3} - \phi) + \frac{\beta\phi}{\upsilon_A N_{Ac}} \ln(\phi/\phi_s) + \frac{(1-\phi)\ln(1-\phi)}{\upsilon_B N_B} + \frac{\chi}{\upsilon_0}\phi(1-\phi) \tag{3}$$

where N_B is the number of units per linear B chain, υ_B is the molar volume per repeat of the B chain, υ_0 is the reference volume of the lattice, and ϕ is the volume fraction of the network (the A component). Note that the free energy of the network is multiplied by the volume fraction of the network in the system, ϕ, before it is added to the terms for the free energy of mixing. Binder and Frisch used a working definition of the chemical potential as $\mu = \partial(\Delta f/kT)/\partial\phi$, which we will forsake for the classical definition $\mu_B = \partial(\Delta F/kT)/\partial n_B$. The volume fraction of the linear chains can be written as $(1-\phi) = n_B\upsilon_B N_B/(\upsilon_A N_A + \upsilon_B n_B N_B)$ where n_B is the number of B chains in the system. The corresponding relation for the volume fraction of the network is $\phi = \upsilon_A N_A/(\upsilon_A N_A + n_B\upsilon_B N_B)$. Substituting these relations into eq 3 for ϕ and $(1-\phi)$, multiplying both sides by the total volume $(\upsilon_A N_A + n_B\upsilon_B N_B)$ to obtain the total free energy, ΔF, and taking $\partial(\Delta F/kT)\partial n_B$ one obtains the chemical potential as

$$\mu_B = \frac{\alpha\phi_s^{2/3}\phi^{1/3}}{\upsilon_A N_{Ac}} - \frac{\beta\phi}{\upsilon_A N_{Ac}} + \frac{\phi}{\upsilon_A N_{Ac}} + \frac{\ln(1-\phi)}{\upsilon_B N_B} + \frac{\chi}{\upsilon_0}\phi^2 \tag{4}$$

It is interesting to note that eq 4 is equivalent to the classical equation for the swelling of a network (made in solution) with a solvent,[16] only here the "swelling" solvent is a linear polymer causing the terms due to the entropy of mixing to be multiplied by $1/N_B$.

The coexistence curve is defined as the point where the chemical potential of the components in the two phases are equal. Normally this is determined by calculating both μ_A and μ_B and writing two equations by setting $\mu_A' = \mu_A''$ and $\mu_B' = \mu_B''$ (the single and double primes indicate the two phases in equilibrium), which are then solved numerically for ϕ' and ϕ''. In our case the situation is simplified because at equilibrium the system contains one phase of pure linear chains in equilibrium with a phase consisting of a network which is swollen with linear chains of component B. The relationship $\mu_B' = \mu_B''$ is then simplified because for the pure phase of linear B chains $\mu_B = 0$. Consequently the coexistence curve can be calculated by setting eq 4 equal to zero. For the case in which the network is polymerized in the presence of the linear chains we make the assumption that the network is relaxed at the polymerization composition so that $\phi_s = \phi$. If we set $\phi_s = \phi$ in eq 4, than it is no longer the equation of the coexistence curve but becomes the cloud-point curve (the point at which the new phase first begins to appear). The actual coexistence curve for a particular system must be calculated from eq 4 by using the value of ϕ_s for the network in question. The equation for the cloud-point curve is then

$$\frac{\phi}{\upsilon_A N_{Ac}}(\alpha - \beta) + \frac{\phi}{\upsilon_B N_B} + \frac{\ln(1-\phi)}{\upsilon_B N_B} + \frac{\chi}{\upsilon_0}\phi^2 = 0 \tag{5}$$

The second derivative of the free energy with respect to composition set equal to zero gives the equation of the spinodal. Taking $\partial^2(\Delta f/kT)/\partial\phi^2 = 0$ yields the spinodal

$$\frac{\partial^2(\Delta f/kT)}{\partial\phi^2} = \frac{-\alpha\phi_s^{2/3}}{3\upsilon_A N_{Ac}\phi^{5/3}} + \frac{\beta}{\upsilon_A N_{Ac}\phi} + \frac{1}{\upsilon_B N_B(1-\phi)} - 2\frac{\chi}{\upsilon_0} = 0 \tag{6}$$

If we assume $\phi_s = \phi$ the equation for the spinodal (valid for systems kept fixed at the polymerization concentration, ϕ) becomes

$$\frac{(\beta - \alpha/3)}{\upsilon_A N_{Ac}\phi} + \frac{1}{\upsilon_B N_B(1-\phi)} - 2\frac{\chi}{\upsilon_0} = 0 \tag{7}$$

The first term in eq 7 is due to the elastic contribution of the network of A chains while the second and third terms are from the free energy of mixing for the linear B chains. Negative terms in eq 7 favor phase separation while positive ones favor phase mixing. The second derivative of the free energy with respect to composition given by eq 7 is proportional to the inverse of the zero-angle scattering intensity, $S(0)^{-1}$, which can be measured by SANS.[21-22]

It is informative to examine the effect of the value of the constant β on the equations for the cloud-point curve and the spinodal given by eq 5 and 7. Assuming $\alpha = 1$, then for values of $\beta > 1$ the cloud-point curve shifts, resulting in an increased single-phase region as N_{Ac} is decreased while $\beta < 1$ results in an increase in the two-phase region of the phase diagram as N_{Ac} is decreased. When $\beta = 1$ the elastic terms in the cloud-point curve cancel and the cloud-point does not depend on N_{Ac} (the system becomes equivalent to a linear blend with one component having infinite molecular weight). The effect of increasing the cross-link density on the spinodal line (eq 7) hinges on a different value of β than the cloud-point curve. For $\beta > {}^1/_3$ the value of χ_s increases with decreasing N_{Ac} (resulting in a smaller unstable region) while for $\beta < {}^1/_3$ the value of χ_s decreases with decreasing N_{Ac}).

Figure 1 is a plot of χN versus ϕ (ϕ is the concentration of the network phase) for eq 5 and 7 ($\phi_s = \phi$) for the special cases where $N_{Ac} = N_B = N$ and $N_{Ac} = \infty$, $N_B = N$ (and $\upsilon_A = \upsilon_B = \upsilon_0$). The constants α and β were chosen to be 1 and ${}^1/_2$ after Flory.[20] For the case $N_{Ac} = N_B = N$ the upper dotted line shows the spinodal while the lowest solid line gives the cloud-point curve. It is clear that the presence of the elastic terms in the free energy causes the downward curve of the cloud-point curve at dilute network concentrations, indicating that even for large negative values of χN the system will be inherently unstable and tend to phase separate. The intermediate set of lines in Figure 1 represent the limiting case of eq 5 and 7 where $N_{Ac} = \infty$ (the dashed curve is the spinodal while the solid one is the cloud-point curve), which is equivalent to the case of a linear blend with one component having infinite molecular weight. By comparison of the two cases it is apparent that the elastic terms in the free energy (choosing $\alpha = 1$ and $\beta = {}^1/_2$) decrease the one-phase region as defined

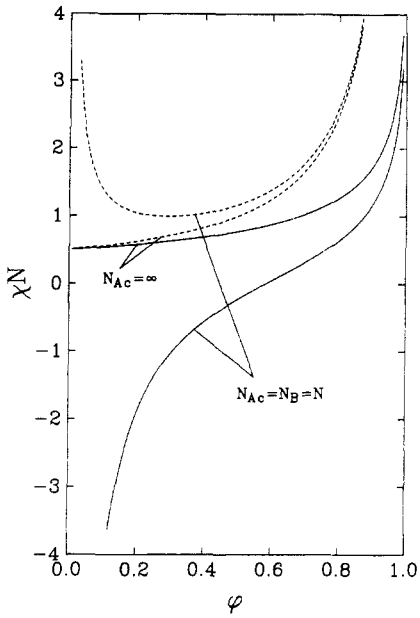

Figure 1. Cloud-point and spinodal curves for two cases of a polymer network (concentration ϕ) polymerized in the presence of a linear polymer, B, (concentration $(1 - \phi)$). Case 1: $N_{Ac} = N_B = N$. Case 2: $N_{Ac} = \infty$, $N_B = N$.

by the cloud-point curve with respect to a linear blend with one infinite molecular weight component while the unstable region defined by the spinodal line is actually increased. If $\beta < {}^1/_3$ this opposite behavior of the cloud-point and spinodal curves no longer occurs and both the cloud point and spinodal shift to lower values of χN with respect to the linear blend. The effect of increasing the cross-link density of the network while keeping the length of the linear chain fixed is to increase separation between the spinodal and the cloud-point curves. For the case of $\beta = {}^1/_2$ the spinodal shifts to larger χ with decreasing N_{Ac} while the cloud point shifts to lower χ. When $\beta < {}^1/_3$, both the spinodal and cloud-point curve shift to lower χ with decreasing N_{Ac}, but the cloud-point curve shifts by a larger amount, increasing the separation between the curves.

Binder and Frisch only examined these effects of the value of β on the phase diagram with respect to the spinodal line which can be slightly misleading. While it is important to note that the spinodal line does show increased stability of the system due to the formation of the network when ${}^1/_3 < \beta < 1$, this is not true for the cloud-point curve. The presence of the network always decreases the single-phase region with respect to the cloud point for all values of $\beta < 1$.

Unfortunately Binder and Frisch did not calculate the entire scattering function, $S(q)$, in their paper. Small-angle scattering studies[9-12] have shown that the scattering function for linear blends can be described quite well by mean-field theories as presented by de Gennes[23] and Benoit et al.[24] In the limit of small q ($q = 4\pi \sin \theta/\lambda$, λ is the wavelength of the scattered radiation) the scattering function for a linear blend in the single-phase region can be approximately by the classical Ornstein–Zernike form

$$S(q) = \frac{S(0)}{1 + \xi^2 q^2} \tag{8}$$

where ξ is the correlation length of the concentration fluctuations present in the blend. It follows that a plot of $S(q)^{-1}$ versus q^2 should be linear with an intercept of $1/S(0)$ and a slope of $\xi^2/S(0)$. The SANS scattering from the systems studied in this paper should follow eq 8 at small q, though there may be deviations at large q. This should allow the extrapolation of SANS data to obtain $S(0)$ and hence $\partial^2(\Delta f/kT)/\partial\phi^2$ and the spinodal temperature.

Table I[a]

sample	ϕ_{PSD}[b]	ϕ_{PSD}[c]	N_{PSD}[b]	N_{cPSD}[d]	Q
1	0.57	0.55			
2	0.45	0.47	900	2040	30.8
3	0.56	0.54	250	380	12.8
4	0.49	0.45	75	100	7.5

[a] ϕ_{PSD}, volume fraction PSD; N_{AC}, number average of repeat units between cross-links; Q, PSD swelling ratio in toluene (volume swollen PSD/volume dry PSD network). [b] Calculated from concentration of monomers charged to reaction. [c] Calculated from carbon elemental analysis. [d] Calculated from swelling ratios in toluene (25 °C).

Experimental Section

Poly(vinyl methyl ether) was synthesized by cationic polymerization with boron trifluoride ethyl ether complex as initiator.[25] The polymerization was done at dry ice temperatures in toluene. The PVME was fractionated with toluene as solvent and heptane as nonsolvent. The PVME had a molecular weight of 633 000 and $M_w/M_n = 1.71$ as measured by gel permeation chromatography (GPC).[26] The PVME was dissolved in toluene and poured into the neutron scattering cell. The cell contained a 1.5 mm thick by 14 mm diameter spacing ring which contained the solution. The toluene was evaporated and more solution was added until half of the cell was filled with PVME. It was then placed in a 70 °C vacuum oven overnight to remove the solvent and any absorbed water.

Styrene-d_8 was dried over calcium hydride and distilled. Divinylbenzene (55–60% active DVC reported) was diluted with toluene to concentrations of approximately 1, 3, and 10% DVB. A 10% solution of azobis(isobutyronitrile) (AIBN) in toluene was made. The styrene-d_8 was added until the level reached the top of the ring in the SANS cell. Four samples were made with one containing no DVB (sample 1) and three others (samples 2–4) which contained one drop of the three different DVB solutions. One drop of AIBN solution was added to each and the cell was assembled. After allowing 24 h for the samples to become uniform, they were placed in a 70 °C oven for 67 h. The cell was then disassembled and the samples were placed in a vacuum oven to remove traces of toluene and monomer. Table I gives the compositions and cross-link densities of the samples studied. The cross-link densities were calculated from the amount of monomers charged assuming 57% active DVB and 100% total conversion.

The neutron scattering was done at the NBS SANS facility under conditions identical with those used in previous work on linear PSD/PVME blends.[9] The wavelength of the incident neutron beam was 6 Å with $\Delta\lambda/\lambda = 20\%$ as determined by using a rotating velocity selector. The data were collected by using a two-dimensional x–y detector and were corrected for scattering from the empty cell, incoherent scattering, and sample thickness and transmission. The scattered intensity was put on an absolute scale by using a calibrated secondary standard of silica gel.

Studies of sample 3 in the deformed state were made by using a copper sample cell which had a groove machined into it. The sample was cut down to fit into the groove and the cell was assembled and compressed. The geometry of the cell constrained the sample to keep its original size in one direction while increasing in size $L/L_0 = 2.5$ in the other direction. The scattering function was then recorded at different temperatures. Because of the anisotropic nature of the scattering, the data were analyzed by performing sector averages over regions 15° wide parallel and perpendicular to the deformation direction.

After the neutron scattering experiments were completed, portions of the four samples were weighed and placed into excess toluene and allowed to reach equilibrium. Sample 1 (0% DVB, uncross-linked) dissolved completely while the other samples only swelled. GPC of sample 1 indicated that the PSD molecular weight was greater than that of PVME. The toluene was exchanged three times and allowed to reequilibrate for samples 2–4 in order to extract the linear PVME chains. GPC on the soluble portions of samples 2, 3, and 4 was similar to that of the starting PVME, indicating that the extractable material was largely

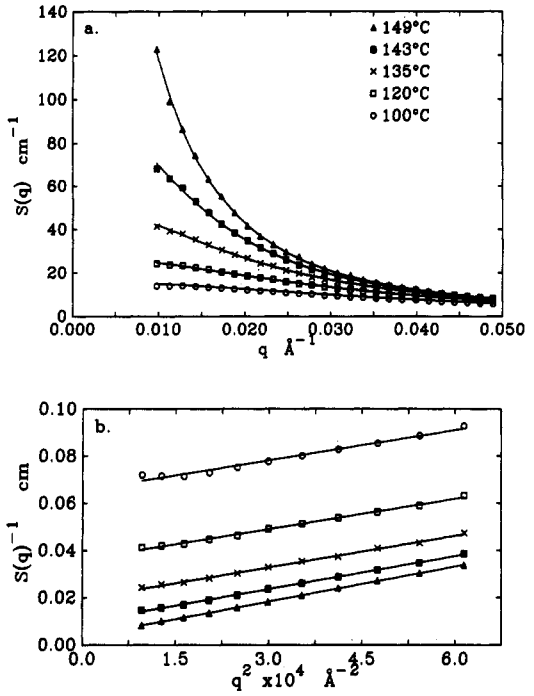

Figure 2. (a) $S(q)$ versus q at a several different temperatures for sample 1 (linear blend). (b) $S(q)^{-1}$ versus q^2 for the same sample.

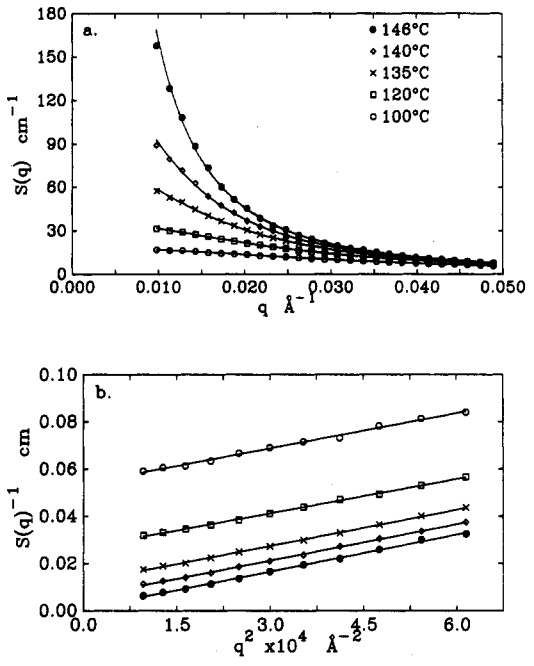

Figure 3. (a) $S(q)$ versus q at a several different temperatures for sample 2. (b) $S(q)^{-1}$ versus q^2 for the same sample.

PVME. Swelling ratios, Q, were calculated from the weight of the sample before it was placed in toluene, taking into account the concentration of PSD in the sample and assuming volume additivity and that all the PVME was extracted from the network. Swelling ratios are presented in Table I. The inverse of the swelling ratios can then be used in eq 4 to calculate the value of N_{Ac} assuming $N_B = 1$. For the case of a gel swollen with a solvent, the lattice volume is taken as the solvent volume so $v_0 = v_B$ (v_B for toluene is 106.3 cm^3/mol). χ was calculated by using the equation $\chi = 0.44 - 0.34\phi$, which was measured by Noda et al. for PS in toluene.[27] The values of N_{Ac} obtained are given in Table I. They differ somewhat from the values calculated from the concentration of DVB added to the polymerization but exhibit the same trends.

Elemental analysis for carbon, oxygen, and hydrogen was performed on the samples to provide a check on the PSD/PVME concentrations calculated from the starting concentration of monomers. The carbon concentration was used to obtain the amount of PSD and PVME present in the blends rather than the oxygen or hydrogen contents, which would be influenced by the presence of absorbed water. The concentrations obtained from the elemental analysis are also presented in Table I and agree reasonably well with the values obtained from the initial monomer concentrations.

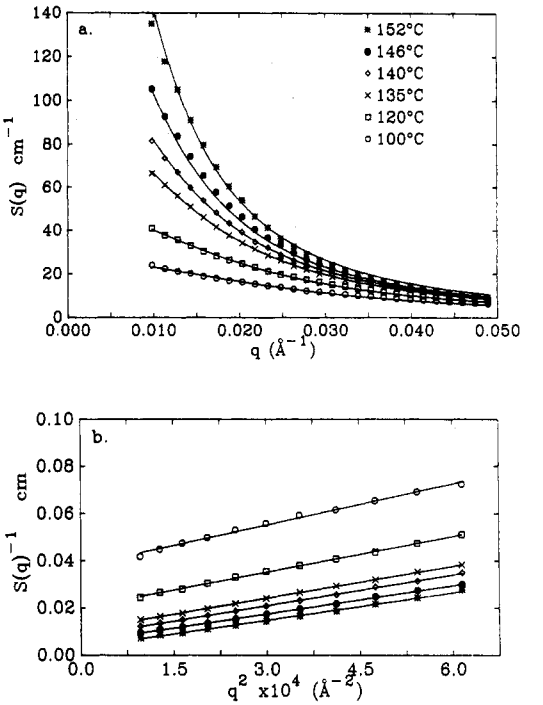

Figure 4. (a) $S(q)$ versus q at a several different temperatures for sample 3. (b) $S(q)^{-1}$ versus q^2 for the same sample.

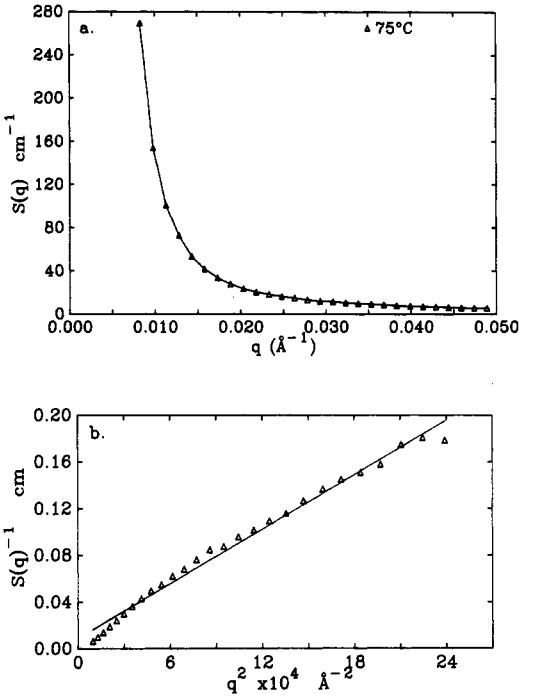

Figure 5. (a) $S(q)$ versus q at a 75 °C for sample 4. (b) $S(q)^{-1}$ versus q^2 for the same sample; the nonlinear behavior of the data is indicating that the sample is phase separated.

Results and Discussion

Figures 2a–5a present the scattering curves $S(q)$ versus q as a function of temperature for samples 1–4, respectively. Figures 2b–4b are plots of $S(q)^{-1}$ versus q^2 (0.009

Table II

	sample 1		sample 2		sample 3	
T, °C	$S(0)$, cm^{-1}	ξ, Å	$S(0)$, cm^{-1}	ξ, Å	$S(0)$, cm^{-1}	ξ, Å
100	15.4	25.7	18.6	30.3	26.4	39.1
120	27.5	34.1	37.3	42.4	50.3	50.6
125	33.0	38.5	42.7	45.6	60.1	54.7
130	40.3	42.4	56.6	57.6	74.2	59.1
135	51.2	47.6	81.4	64.0	94.5	65.2
140	78.1	59.9	167.4	92.1	125.1	73.4
143	102.4	68.6	278.3	118.0	151.0	80.1
146	144.5	82.6	898.5	214.7	179.0	84.0
149	281.5	117.7			227.7	94.0
152					281.6	102.5

Table III

orig temp, °C	new temp,[a] °C	orig temp, °C	new temp,[a] °C
100	104	135	138
120	124	140	143
125	129	143	146
130	134	146	149

[a] Determined by using eq 12 with the values T_1 = old temperture, T_2 = new (shifted) temperature, $\phi_1 = 0.47$, $\phi_2 = 0.55$, $C_1 = 8.714 \times 10^{-4}$, $C_2 = 4.749 \times 10^{-4}$, $C_3 = -3.543 \times 10^{-1}$, and $C_4 = -2.461 \times 10^{-1}$.[31]

$\leq q \leq 0.025$ Å^{-1}) for samples 1–3, respectively, as a function of temperature. The lines drawn through the data in Figures 2b–4b are linear least-squares fits to the data. The plots are linear, indicating that the scattering fits the functional form given by eq 8. The straight line fit to the data allows extrapolation to $q = 0$, which gives a value for $S(0)$, the scattered intensity at zero angle. From the square root of the ratio of the slope to the intercept, the correlation length, ξ, can be calculated. The curves drawn through the data in Figures 2a–4a are calculated by using eq 8 and the values of $S(0)$ and ξ given in Table II.

Figure 5b shows the plot of $S(q)^{-1}$ versus q^2 (at 75 °C) for sample 4, which contained the largest amount of DVB. The plot is clearly nonlinear. This indicates that the sample phase separated at the temperature of polymerization (70 °C). Upon closer examination, after the SANS experiments were completed, a faint cloudiness could be observed when the sample was held up to the light. The sample remained phase separated after annealing for 12 h at 75 °C and then at 100 °C, conditions which would have returned a linear PSD/PVME blend to the homogeneous state.

It has been argued theoretically[28,29] and demonstrated experimentally[9–12] that the phase-separation behavior of polymer blends follows mean-field behavior. As the spinodal is approached the zero-angle scattering and correlation length should diverge as

$$S(0) \sim (\chi_s - \chi)^{-\gamma} \tag{9}$$

and

$$\xi \sim (\chi_s - \chi)^{-\nu} \tag{10}$$

where $\gamma = 1$ and $\nu = {}^1/_2$ for a mean-field system.[30] Assuming the Flory interaction parameter varies as $1/T$, $(\chi_s - \chi) \sim (T_s^{-1} - T^{-1})$, implying that $S(0)^{-1}$ and ξ^{-2} should vary linearly with inverse temperature.

Before plotting the zero-angle scattering and the correlation length, it should be noted that the composition of sample 2 is significantly different than the composition of the other two homogeneous samples (samples 1 and 3). This makes it difficult to compare it to the other two samples because of the known concentration dependence

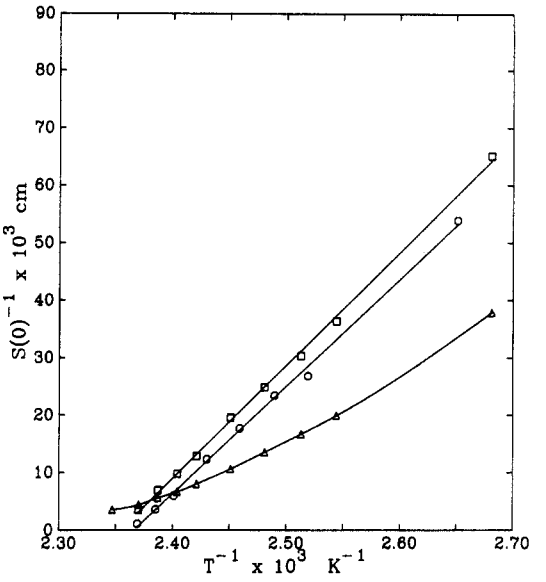

Figure 6. $S(0)^{-1}$ versus T^{-1} for sample 1 (squares), sample 2 (circles), and sample 3 (triangles).

of the interaction parameter.[9–12,31] The functional form of χ obtained from SANS can be written as

$$\frac{\chi}{v_0} = C_1 + C_2\phi + \frac{C_3 + C_4\phi}{T} \tag{11}$$

where T is the absolute temperature, ϕ is the volume fraction of PSD, and C_1, C_2, C_3 and C_4 are constants.[31] By use of values of C_1, C_2, C_3, and C_4 obtained for PSD/PVME and with constant χ/v_0 assumed, the concentration difference of sample 2 can be accounted for by calculating a new set of temperatures to correspond to the data for sample 2 normalized to a PSD content of 0.55 (the volume fraction of PSD in sample 1) according to eq 12; where ϕ

$$C_2\phi_1 + \frac{C_3 + C_4\phi_1}{T_1} = C_2\phi_2 + \frac{C_3 + C_4\phi_2}{T_2} \tag{12}$$

and T_1 are the original temperatures and starting composition ($\phi_1 = 0.47$) and T_2 and ϕ_2 are the new temperatures at the new composition ($\phi_2 = 0.55$, the same as for sample 1). The values of C_1, C_2, C_3, and C_4 were obtained from ref 29 and are given in Table III along with the new shifted temperatures. The data for sample 3 was not shifted from $\phi = 0.54$ to $\phi = 0.55$ because the resulting new temperatures in this case would not be significantly different from the original ones.

The shifting of the data for composition differences based on values of χ determined from previous experiments with blends of linear PSD and PVME assumes that the composition dependence of χ is equivalent between the linear system and the one studied in this work. This procedure should be qualified somewhat because there is some evidence that χ is not the same for the two systems. The spinodal temperature measured for the linear blend in this paper is somewhat lower (7–10 °C) than would be expected on the basis of past experiments with linear materials even when the very high molecular weights used in this work are taken into account. This could be ascribed to the fact that the PSD in this work was made by a free radical polymerization while the previous work was done with anionically polymerized PSD. These differences could result in tacticity changes between the samples which has been shown to have strong effects on the phase diagrams of other polymer systems.[32]

Figures 6 and 7 are plots of $S(0)^{-1}$ and ξ^{-2} versus T^{-1} for sample 2 (plotted with the shifted temperatures) along

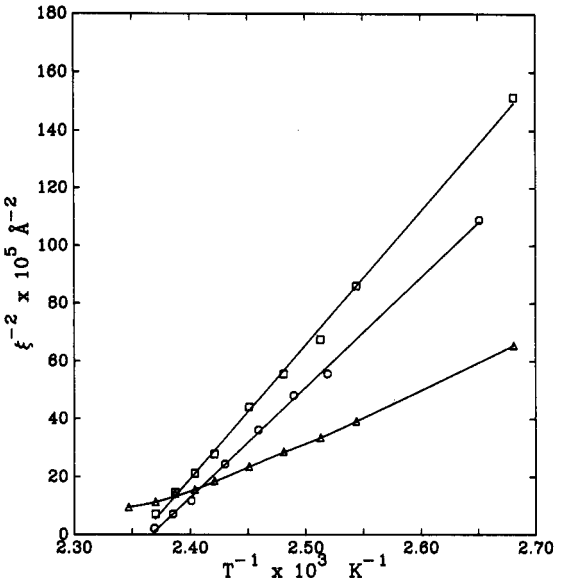

Figure 7. ξ^{-2} versus T^{-1} for sample 1 (squares), sample 2 (circles), and sample 3 (triangles).

with the data for samples 1 and 3. The squares in Figures 6 and 7 are data from sample 1 which exhibit linear behavior as expected for a linear polymer blend. The lines drawn through the squares in Figures 6 and 7 are linear least-squares fits to the data (based on eq 9 and 10) which allows extrapolation to the spinodal temperature, T_s, where $S(0)^{-1}$ and ξ^{-2} equal zero. The extrapolation gives T_s = 152 °C and 151 °C using $S(0)^{-1}$ and ξ^{-2}, respectively. The circles in Figures 6 and 7 are data for sample 2 and the triangles are for sample 3.

At low temperatures (~100 °C) the data all show a consistent trend; with increasing crosslink density the inverse zero-angle scattering and ξ^{-2} decrease (increasing long-wavelength fluctuations). This imples that at 100 °C (and presumably at the polymerization temperature of 70 °C) increasing the cross-link density brings the system closer to the spinodal line. This is also consistent with the results from sample 4 which indicate that if the cross-link density is increased significantly above the level present in sample 3 the system will phase separate during the polymerization. The cross-link density present in sample 4 has clearly exceeded the value that would correspond to equilibrium swelling with a ratio of $Q \simeq 2$ (Q = the inverse volume fraction of PSD in the sample), which then leads to phase separation.

The behavior of $S(0)^{-1}$ and ξ^{-2} with temperature is more complicated for samples 2 and 3 then for sample 1. The plot of $S(0)$ versus $1/T$ for sample 2 (circles in Figures 6 and 7) shows a linear relationship similar to sample 1, only with a different intercept. If the linear relationship in Figures 6 and 7 is assumed to hold up to the spinodal for sample 2, the values of T_s evaluated from $S(0)$ and ξ are found to be the same with T_s = 150 °C. Sample 3 on the other hand, behaves qualitatively different (see triangles in Figures 6 and 7). With increasing temperature the value of $S(0)^{-1}$ for sample 3 starts off smaller than that for the other homogeneous samples but then does not decrease as rapidly and eventually crosses over the values for samples 1 and 2.

At low temperatures, the behavior of $S(0)^{-1}$ with increasing cross-link density is what would be expected from eq 7 with $\beta < 1/3$; as the density of the network increases at a fixed polymerization temperature the system approaches the spinodal. Sample 4 probably never reached the true spinodal but phase separated during the polymerization when the system crossed over the cloud-point curve.

The fact that the curve of $S(0)^{-1}$ versus T^{-1} crosses over that for the linear blend indicates that the value of β may be changing with temperature and that at the point of intersection of the curves for samples 1 and 3 (at 146 °C) the value of β equals $1/3$. In addition, the plot of $S(0)^{-1}$ versus T^{-1} is curved for sample 3, indicating that the simple model presented for the zero-angle scattering discussed above is no longer valid. Either the formulation of the free energy of the network used in determining the total free energy needs to be examined more carefully or the system may be deviating from the mean-field behavior implicit in the model.

In discussing the data it is interesting to note that at high temperatures, close to or above where the linear blend would phase separate, the long-wavelength concentration fluctuations for sample 3 are significantly damped. The network nature of the PSD phase, while pushing the system toward phase separation during the polymerization by limiting the entropy gain from the mixing of the PVME chains (because of the opposing loss of free energy due to the stretching of the PSD network), reverses its behavior (if the sample is successfully polymerized without phase separation) and effectively constrains the concentration fluctuations to be smaller than would be present in a linear blend when the temperature is raised. This causes the plots of $S(0)^{-1}$ and ξ^{-2} versus T^{-1} for sample 3 to curve at high temperatures. One explanation for the lack of curvature in Figures 6 and 7 for sample 2 as compared with sample 3 is that the dominant wavelength of the concentration fluctuations must become larger than some average size, related to the mesh size of the network, to be damped by the network nature of the PSD phase. The curve for sample 3 crosses that for sample 1 at about 146 °C in Figure 7, which corresponds to a correlation length of about 84 Å. If the length scale at which the PSD network begins to influence (and damp) the concentration fluctuations scales with the square root of the number of units cross-links, $N_{Ac}^{1/2}$, then the curve of ξ^{-2} versus T^{-1} for sample 2 can be estimated to cross that for sample 1 at a correlation length of 160 Å (as compared to 84 Å in sample 3). There is only one data point (at 146 °C) that has a correlation length larger than 160 Å for sample 2, making the crossover for sample 2 difficult to observe. Unfortunately data were not obtained at temperatures higher than 146 °C for sample 2.

The question also arises as to whether the scattering obtained for sample 3 was from a system in equilibrium and not changing with time. To address this question one of the data points at a lower temperature for sample 3 was repeated after the data at higher temperatures were collected. The curvature in the plot of $S(0)^{-1}$ versus T^{-1} was still apparent in the data. Additional evidence supporting the equilibrium nature of the data for sample 3 is that as the scattering data were collected the total scattering intensity was monitored. The total scattering increased for about 10–15 min after the temperature was raised and then leveled off. The data collection was not initiated until this plateau was reached. In addition, the total scattering did not vary significantly during the course of the experiment after data collection was initiated at a given temperature.

The data for sample 3 can also be replotted by using different exponents than the mean-field values assumed in Figures 6 and 7 to obtain a linear relation with inverse temperature. The exponents $1/\gamma$ and $1/\nu$ for $S(0)$ and ξ, respectively, were varied to give the best correlation coefficient in a linear least-squares fit of the form $S(0)^{-1/\gamma}$

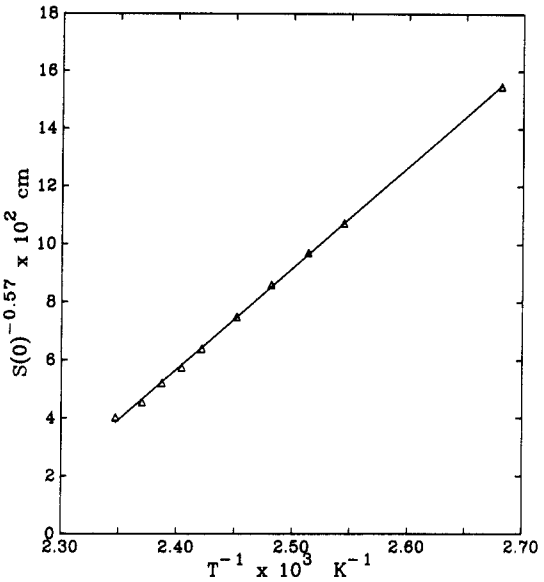

Figure 8. $S(0)^{-0.57}$ versus T^{-1} for sample 3, which gives a linear relationship.

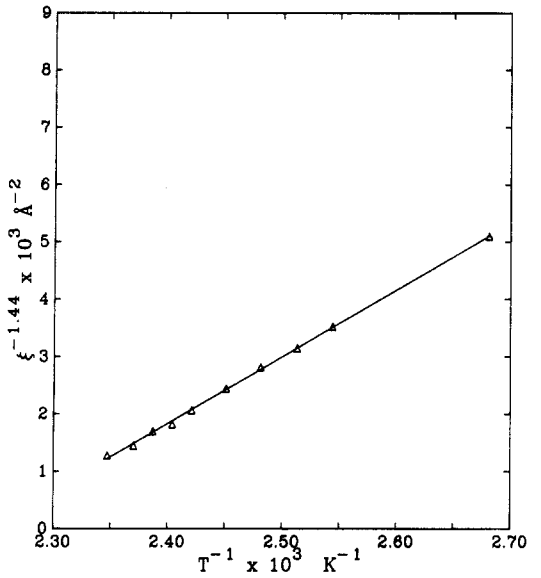

Figure 9. $\xi^{-1.44}$ versus T^{-1} for sample 3, which gives a linear relationship.

or $\xi^{-1/\nu}$ versus T^{-1}. Figures 8 and 9 show the data for $S(0)$ and ξ plotted versus T^{-1} by using the exponents $1/\gamma = 0.57$ and $10/\nu = 1.44$, respectively, which gave the best fit. The straight lines in figures 8 and 9 are the linear fits to the data. The data presented in Figures 8 and 9 show linear behavior with the exponents chosen, but the fit is not very sensitive to the value of the exponents. Whether this method of plotting the data is valid remains to be seen, but it is clear from the data for sample 3 that $S(0)$ and ξ do not diverge as quickly as in the linear blend as T approaches T_s. From the plots presented in Figures 8 and 9, the spinodal temperatures based on the $S(0)$ and ξ can be estimated. The two plots give the same T_s of 173 °C, approximately 20 °C higher than is observed for the linear blend.

Sample 3 was placed in the deformation cell and deformed by a factor of $L/L_0 = 2.5$ in one direction, while being constrained to keep the original dimension in the perpendicular direction in the plane perpendicular to the incident neutron beam. The SANS data were collected immediately after deformation of the sample. While the linear chains in the sample were probably not relaxed,

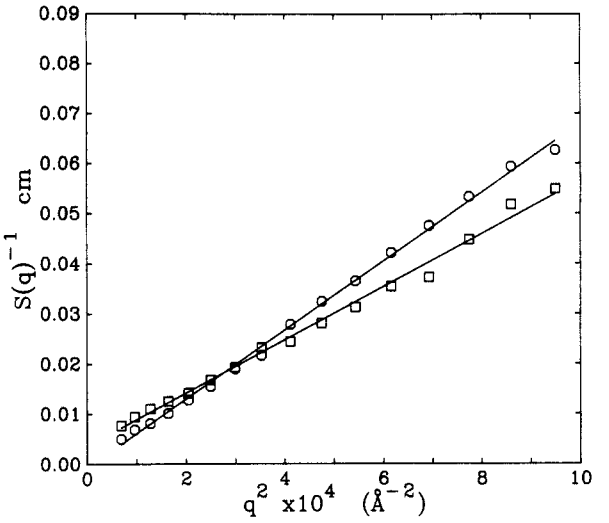

Figure 10. $S(q)^{-1}$ versus q^2 for deformed sample 3 at 140 °C. Circles, parallel to the deformation; squares, perpendicular to the deformation.

there was no time dependence of the SANS data observed over the course of the experiment. The data were averaged over 15° sectors both parallel and perpendicular to the deformation direction. Figure 10 shows a typical plot of $S(0)^{-1}$ versus q^2 ($0.009 \leq q \leq 0.025$ Å^{-1}) for the two directions at a temperature of 140 °C. The scattering in the two directions is clearly different, with the perpendicular direction having a larger intercept and lower slope than the parallel direction. The data for the two directions actually cross in the q range measured in the experiment. This result should be contrasted with the recently published results for poly(dimethylsiloxane) (PDMS) networks swollen with linear deuterated PDMS chains where the scattering was found to be isotropic, with the scattering function of the linear chains following Gaussian behavior at deformations up to $L/L_0 = 1.45$.[33] The linear chains in the PDMS study were the same length as the chain length between cross-links, while in the sample discussed in this paper the linear chains are on the order of 30 times larger than the length between cross-links. One might expect the linear chains in the sample discussed in this paper to be more strongly entangled with the network than in the case with the PDMS chains.

The intercept in Figure 10 is proportional to the distance the sample is away from the spinodal in terms of $(\chi_s - \chi)$. As the temperature approaches the spinodal temperature the data in the two directions shift forming a family of lines with decreasing intercepts (see Figures 2b–4b for the undeformed samples as examples). The correlation length can be calculated in the same manner as for the undeformed samples (as the square root of the ratio of the slope to the intercept). The differing intercepts and slopes of the two curves in Figure 10 indicate that the sample is approaching two different spinodal temperatures in the parallel and perpendicular directions, with T_s in the parallel direction occurring first.

Figures 11 and 12 are the plots of $S(0)^{-1}$ and ξ^{-2} versus T^{-1} for the deformed sample. The uncertainties in the data presented in Figures 11 and 12 are greater than for the isotropic samples for a number of reasons. The fact that the scattering is anisotropic disallows the circular averaging, which improves the signal-to-noise ratio in the isotropic samples. In addition, the scattered intensity from the deformed samples is much lower than from the isotropic samples because of the considerable attenuation (about 50%) from the copper deformation cell and the

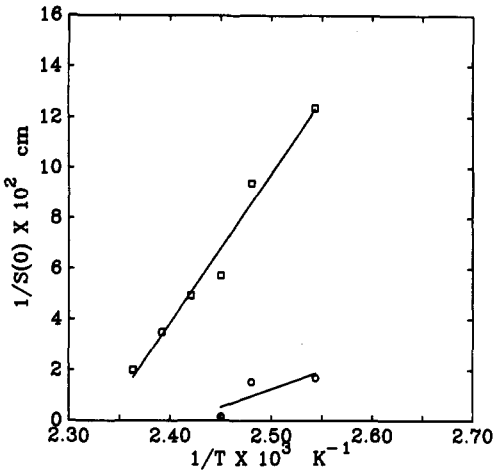

Figure 11. $S(0)^{-1}$ versus T^{-1} for deformed sample 3. Circles, parallel to the deformation; squares, perpendicular to the deformation. Note that the perpendicular direction has a lower T_s.

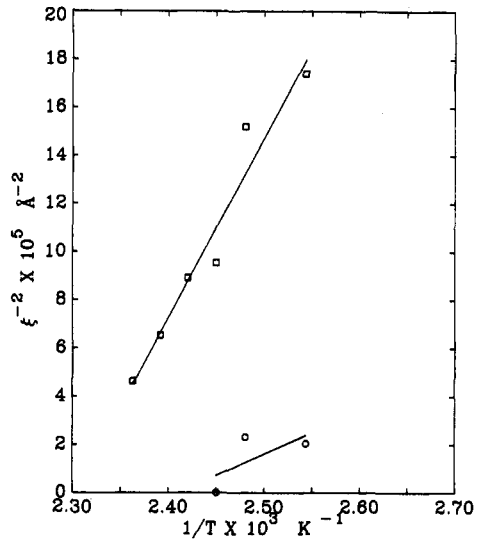

Figure 12. ξ^{-2} versus T^{-1} for deformed sample 3. Circles, parallel to the deformation; squares, perpendicular to the deformation. Note that the perpendicular direction has a lower T_s.

smaller scattering volume of the deformed sample (due to the thinning of the sample that occurs during the deformation). It was not possible to determine whether there is curvature in the data in Figures 11 and 12 so the choice of the exponents for $S(0)$ and ξ was not clear for the deformed sample. The spinodal temperatures determined from $S(0)^{-1}$ for the parallel and perpendicular directions were 141 and 155 °C, respectively, while the spinodal temperatures determined from ξ^{-2} were 142 and 161 °C for the parallel and perpendicular directions. When the $S(0)$ and ξ data for the deformed sample are plotted as $S(0)^{-0.57}$ or $\xi^{-1.44}$ versus T^{-1}, approximately the same T_s is obtained in the direction perpendicular to the deformation (the values of T_s perpendicular were 169 and 171 °C, respectively) as was obtained for the undeformed sample. In the parallel direction, changing the value of the exponents had little effect on the value of T_s (141 and 146 °C, respectively).

There are only three data points for the direction parallel to the deformation because at the higher temperatures the $S(q)^{-1}$ versus q^2 plots gave negative intercepts, indicating that the sample had phase separated in this direction while apparently remaining single phase in the perpendicular direction. The data clearly demonstrate that the spinodal temperature is lowered significantly in the direction parallel to the deformation, while remaining roughly equivalent to the undeformed sample in the perpendicular direction. One possible explanation for this result is the system is forming domains which are oriented with their long axis perpendicular to the deformation, giving rise to the prominent concentration fluctuations along the deformation direction while remaining more homogeneous in the opposite direction. A mean-field theory recently presented to describe the effect of a flow field on the phase-separation transition for polymer systems predicts that the spinodal temperature should not be shifted (within the mean-field framework of the model) but there should be observable anisotropy in the scattering function in the one-phase region.[34]

Conclusions

Single-phase samples of cross-linked PSD containing about 50% linear high molecular weight PVME have been synthesized by dissolving the PVME in a mixture of styrene-d_8 and divinylbenzene which is subsequently polymerized. If the cross-link density of the PSD phase is increased beyond the level that can support an equilibrium swelling of the PSD network by 50% PVME, the sample phase separates during the polymerization. The cross-link density where phase separation occurs is lower than would be observed for a low molecular weight solvent because of the much lower entropy of mixing that occurs when a network is swollen with a polymer than when it is swollen with a solvent. For the system studied in this paper phase separation occurs as the number of repeat units between crosslinks, N_{Ac}, for the PSD network is lowered from 380 to 100 units. This is for a system that was polymerized at 70 °C with about 50% by weight of 633 000 molecular weight PVME.

The samples that were successfully polymerized without phase separation were studied by SANS as a function of temperature. At low temperatures, the samples exhibited increased zero-angle scattering and correlation length with increasing cross-link density with respect to the linear blend. However, this behavior was not retained by the highest cross-link-density sample (sample 3) as the temperature was increased. The zero-angle scattering and correlation length for sample 3 did not increase as fast with increasing temperature as did $S(0)$ and ξ for the lower cross-link-density sample (sample 2) or the linear sample (sample 1) with $S(0)$ and ξ for sample 3 eventually crossing over the curves for the other two samples at 146 °C. The plots of $S(0)^{-1}$ and ξ^{-2} versus T^{-1}, which were linear for the linear and lowest cross-link density samples, exhibited pronounced curvature for sample 3. This curvature resulted in sample 3 actually exhibiting a larger single-phase region than the corresponding linear blend. This curvature could possibly be explained by a temperature dependence of the constant β, associated with the logarithmic term in the free energy for deformation of a network, and/or by a deviation from the classical mean-field exponents for $S(0)$ and ξ usually associated with polymer blends. Linear plots for the zero-angle scattering and the correlation length versus T^{-1} could be obtained for sample 3 with the exponents $S(0)^{-0.57}$ and $\xi^{-1.44}$.

A deformation experiment was performed with sample 3 by compressing the sample in a die which constrained the lateral dimension to remain constant while increasing the length of the sample by the factor $L/L_0 = 2.5$. The SANS from this deformed sample was anisotropic, resulting in different values of $S(0)$ and ξ in the parallel and perpendicular directions. Plots of $S(0)^{-1}$ and ξ^{-2} versus T^{-1} indicated that the sample phase separated in the direction parallel to the deformation at a lower temperature than

in the perpendicular direction. This could be associated with the formation of highly anisotropic domains perpendicular to the deformation direction.

Acknowledgment. We wish to thank Drs. C. Glinka and J. Gotaas at the National Bureau of standards for help with the SANS experiments.

Registry No. (DVB)(S) (copolymer), 9003-70-7; PVME, 9003-09-2; neutron, 12586-31-1.

References and Notes

(1) Bauer, B. J.; Briber, R. M.; Han, C. C. *Polym. Prepr. (Am. Chem. Soc., Div. Polym. Chem.)* **1987**, *28*(2), 169.
(2) Briber, R. M.; Bauer, B. J. *Macromolecules*, in press.
(3) Sperling, L. H. *Interpenetrating Polymer Networks and Related Materials*; Plenum: New York, 1981.
(4) Sperling, L. H. In *Multicomponent Polymer Materials*; Paul, D. R., Sperling, L. H., Ed.; Advances in Chemistry 211; American Chemical Society: Washington, DC, 1986; Chapter 2.
(5) Kim, S. C.; Klempner, D.; Frisch, K. C.; Frisch, H. L.; Radigan, W. *Macromolecules* **1976**, *9*, 258.
(6) Frisch, H. L.; Klempner, D.; Yoon, H. K.; Frisch, K. C. *Macromolecules* **1980**, *13*, 1016.
(7) MacKnight, W. J.; Karasz, F. E.; Fried, J. R. In *Polymer Blends*; Paul, D. R., Newman, S., Eds.; Academic Press: New York, 1978.
(8) Coleman, M. M.; Serman, C. J.; Painter, P. C. *Macromolecules* **1987**, *20*, 226.
(9) Han, C. C.; Okada, M.; Muroga, Y.; McCrackin, F. L.; Bauer, B.; Tran-Cong, Q. *J. Polym. Eng. Sci.*, **1986**, *26*, 2.
(10) Shibayama, M.; Yang, H.; Stein, R. S.; Han, C. C. *Macromolecules* **1985**, *18*, 2179.
(11) Jelenic, J.; Kirste, R. G.; Oberthur, R. C.; Schmitt-Streker, S.; Schmitt, B. J. *Makromol. Chem.* **1984**, *185*, 129.
(12) Herkt-Maetsky, C.; Schelten, J. *Phys. Rev. Lett.* **1983**, *51*, 896.
(13) Binder, K.; Frisch, H. L. *J. Chem. Phys.* **1984**, *81*, 2126.
(14) Flory, P. J. *J. Chem. Phys.* **1941**, *9*, 660; **1942**, *10*, 51.
(15) Huggins, M. L. *J. Chem. Phys.* **1941**, *9*, 440.
(16) Dusek, K.; Prins, W. *Adv. Polym. Sci.* **1969**, *6*, 1.
(17) James, H.; Guth, E. *J. Chem. Phys.* **1947**, *15*, 669.
(18) Hermans, J. J. *J. Polym. Sci.* **1962**, *59*, 197.
(19) Kuhn, W. *J. Polym. Sci.* **1946**, *1*, 183.
(20) Flory, P. J. *J. Chem. Phys.* **1950**, *18*, 108.
(21) Smoluchowski, M. *Ann. Phys.* **1908**, *25*, 205.
(22) Einstein, A. *Ann. Phys.* **1910**, *33*, 1275.
(23) de Gennes, P.-G. *Scaling Concepts in Polymer Physics*; Cornell University Press: Ithaca, NY, 1979.
(24) Benoit, H.; Benmouna, M. *Macromolecules* **1984**, *17*, 535.
(25) Certain equipment, instruments, or materials are identified in this paper in order to adequately specify the experimental details. Such identification does not imply recommendation by the National Bureau of Standards nor does it imply the materials or equipment identified are necessarily the best available for the purpose.
(26) Bauer, B. J.; Hanley, B.; Muroga, Y., unpublished results.
(27) Noda, I.; Higo, Y.; Ueno, N.; Fujimoto, T. *Macromolecules* **1984**, *17*, 1055.
(28) de Gennes, P.-G. *J. Phys. Lett.* **1977**, *38*, L441.
(29) Joanny, J. F. *J. Phys. A: Math. Gen.* **1978**, *11*, L117.
(30) Stanley, H. E. *Introduction to Phase Transition and Critical Phenomena*; Oxford University Press: New York, 1971.
(31) Han, C. C.; Bauer, B. J.; Clark, J. C.; Muroga, Y.; Matushita, Y.; Okada, M.; Tran-Cong, Q., submitted for publication in *Polymer*.
(32) Roerdink, E.; Challa, G. *Polymer* **1980**, *21*, 1161.
(33) Boué, F.; Farnoux, B.; Bastide, J.; Lapp, A.; Herz, J.; Picot, C. *Europhys. Lett.* **1986**, *1*, 637.
(34) Fredrickson, G. H. *J. Chem. Phys.* **1986**, *85*, 5306.

Solid State of Cross-Linked Macromolecules: Basic Concepts

Paul Goldbart*,† and Nigel Goldenfeld†,‡

Department of Physics, University of Illinois at Urbana-Champaign, 1110 West Green Street, Urbana, Illinois 61801, and Department of Applied Physics, Stanford University, Stanford, California 94305. *Received November 24, 1987; Revised Manuscript Received June 17, 1988*

ABSTRACT: We present a simple physical picture of the way in which topological entanglements enter into a statistical mechanical theory for the solid state of randomly cross-linked macromolecules. Our approach, which does not require the use of invariants, focuses on the way in which the system explores its phase space. We summarize the results of a detailed calculation and briefly discuss their experimental consequences.

1. Introduction

It has long been recognized that cross-linked systems of flexible macromolecules pose extraordinary difficulties for statistical mechanics. These difficulties result from the combination of two factors: the chainlike nature of the molecules and the presence of permanent cross-links between the chains. These same two factors are also believed to be responsible for the spectacular elastic response of cross-linked systems such as gels and rubber.

We believe that a prerequisite for a genuine statistical mechanical theory of the elastic response of these systems is a sound understanding of the undeformed solid state. This paper is intended to explain the physical considerations underlying our recently proposed theory of the liquid-to-solid transition in cross-linked macromolecules.[1]

Although much has been understood about gels and rubbers from a phenomenological point of view,[2] a genuine microscopic theory must confront the topological complexity of cross-linked systems. The basic problem can be easily seen from Figure 1. Figure 1a shows a portion of a cross-linked system, where two chains, labeled A and B, are cross-linked to the network in such a way that chain A lies in front of chain B. The chains cannot pass through each other or the rest of the network. Consequently, it is impossible, as the system undergoes its dynamics, for the chains to move into the configuration depicted in Figure 1b. In this configuration, chain B lies in front of chain A, yet the chains are cross-linked at precisely the same points as in Figure 1a. The two configurations are said to be topologically inequivalent; if the system is formed in the configuration of Figure 1a, it will always preserve the topological relationships between the chains. A network of

† University of Illinois at Urbana-Champaign.
‡ Stanford University.

0024-9297/89/2222-0948$01.50/0